JOC Article

Ring Currents in Tangentially p−p Bonded σ-Aromatic Systems

Patrick W. Fowler,*,† Agnieszka Rogowska,‡ Alessandro Soncini,§ Mark Lillington,† and Leif P. Olson*,#

Department of Chemistry, University of Sheffield, Sheffield, S3 7HF, United Kingdom, Department of Chemistry, University of Warsaw, Al. Zwirki i Wigury 101, PL 02-089 Warsaw, Poland, Afdeling Kwantumchemie, Departement Chemie, Katholieke Universiteit Leuven, Celestijnenlaan 200F, B-3001 Heverlee, Belgium, and Eastman Kodak Research Laboratories, 1999 Lake Avenue, Rochester, New York 14650

P.W.Fowler@sheffield.ac.uk

Received April 13, 2006

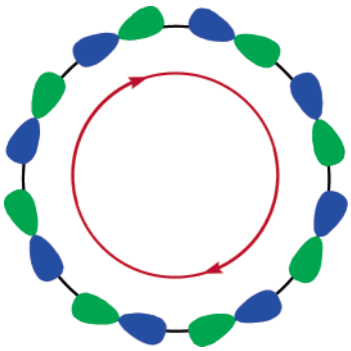

We report a theoretical study of ring systems that delocalize electrons in a cyclic array of p orbitals arranged tangentially in σ-bonding fashion. σ-Bonded arrays are compared to conventional π-bonded analogues with respect to orbital symmetry and aromatic/antiaromatic behavior. In a one-to-one correspondence between π and tangential molecular orbitals of a cycle, local rotation turns each π to a tangential basis function, changing bonding interactions to antibonding and inverting the order of filling of molecular orbitals. The ipsocentric ring-current mapping approach is used to evaluate aromaticity on the magnetic criterion. As for conventional π-ring currents, the σ-ring current in tangential p−p bonded systems is dominated by the HOMO−LUMO transition, corresponding to circulation of four electrons in diatropic $(4n + 2)$-electron cycles but two in paratropic $(4n)$-electron cycles. The systems examined here utilize either C 2p or Si 3p orbitals for delocalization. Although interchangeable with C with respect to the fundamental orbital symmetry and ring-current rules, Si bonds at greater internuclear distances, a feature that allows easier design of potentially stable σ-aromatic structures. Calculations show the wheel-like $Si_{10}C_{50}H_{70}$ structure **6** as a stable, neutral aromatic molecule with a diatropic ring current following the σ-bond path formed by Si 3p orbitals.

Introduction

Theoretical studies of s aromatic or potentially s aromatic cluster ions have steadily appeared over recent years.[1] These ions may be divided into small 2σ-electron systems such as H_3^+ and Li_3^+ where aromaticity (if present) is based on s orbitals[1a,b] and more complicated systems, exemplified by Al_4^{2-}, where the aromaticity has been variously described as σ, π, or even mixed σ/π.[1c−h] For these systems, reliable ring-current mapping

* Corresponding author. Tel.: +44 114 222 9538.
† University of Sheffield.
‡ University of Warsaw.
§ Universiteit Leuven.
# Eastman Kodak Research Laboratories.

(1) (a) Alexandrova, A. N.; Boldyrev, A. I. *J. Phys. Chem. A* **2003**, *107*, 554. (b) Havenith, R. W. A.; De Proft, F.; Fowler, P. W.; Geerlings, P. *Chem. Phys. Lett.* **2005**, *407*, 391. (c) Li, X.; Kuznetsov, A. E.; Zhang, H.-F.; Boldyrev, A. I.; Wang, L.-S. *Science* **2001**, *291*, 859. (d) Kuznetsov, A. E.; Boldyrev, A. I.; Li, X.; Wang, L.-S. *J. Am. Chem. Soc.* **2001**, *123*, 8825. (e) Kuznetsov, A. E.; Corbett, J. D.; Wang, L.-S.; Boldyrev, A. I. *Angew. Chem., Intl. Ed.* **2001**, *40*, 3369. (f) Fowler, P. W.; Steiner, E.; Havenith, R. W. A. *Chem. Phys. Lett.* **2001**, *342*, 85. (g) Fowler, P. W.; Havenith, R. W. A.; Steiner, E. *Chem. Phys. Lett.* **2002**, *359*, 530. (h) Zhan, C.-G.; Zheng, F.; Dixon, D. A. *J. Am. Chem. Soc.* **2002**, *124*, 14795.

10.1021/jo060788p CCC: $33.50
Published on Web 07/19/2006

techniques[2] have been used to establish aromaticity, antiaromaticity, or the lack thereof. A benefit of this approach is that specific orbital contributions to the ring current can be identified, thereby revealing which sets of electrons (σ or π) are magnetically active. Among the interesting findings of the ring-current studies is that diatropic and paratropic circulations can lead to aromaticity phenomena that may contradict or amplify simple electron counting rules.[1]

Theoretical research on aromaticity in organic molecules is generally dominated by studies of the many subtleties of π-electron delocalization in, for example, benzenoid molecules, porphyrins, and so on. Ring-current mapping has shown great explanatory power for the π-aromaticity of organic molecules and has the potential to do likewise for σ-aromaticity where present. σ-Aromaticity is not much considered in organic chemistry. Notable exceptions are in accounts of the electronic structure of cyclopropane and related ring systems,[3] where σ-aromaticity has been invoked, and of mixed σ/π aromaticity in certain homoaromatic[4] molecules or ions and certain pericyclic transition states[5] (although the degree to which long-range overlap of p orbitals in such systems is of a σ- or π-type is not always given any particular attention).

Here, we investigate σ-aromaticity based solely on p orbitals interacting end-to-end in a σ-fashion that may lead to electron delocalization and ring currents. The fundamental building blocks we use are those typical of π-aromatic systems, namely, planar or near-planar three-coordinate sp^2-hybridized atoms (C or Si, the latter having practical advantages, as explained later). The simplest example is a set of eight trigonal-planar CH_3 groups arranged to form a C−C bonded ring. Using DFT theory and ring-current mapping techniques, we examine the electronic structure that results from arranging these units in tangential p−p bonding arrays (Figure 1). We focus particularly on the symmetry properties of the σ-delocalized MOs, the ability of tangential p−p bonds to support a ring current, the ring-current circulation patterns (including contributions from specific MOs), and the nature of the diatropic and/or paratropic excitations that may form σ-aromatic or σ-antiaromatic ring currents. An additional goal of the work was to design a potentially real σ-aromatic molecule (i.e., without using symmetry constraints to enforce the desired orbital interactions). Particularly interesting would be such a molecule that was also electrically neutral, so that it did not rely on charge dispersal to aid aromatic delocalization.

Electron delocalization through a chain of end-to-end p orbitals (or end-to-end d_{z^2} orbitals) is not a new concept.[6] The structures in the present work are cyclic variants of structures previously proposed for the σ-allyl cation,[7] a linear species. Theory indicates that a fully delocalized $[Si-Si-Si]^+$ σ-allyl array may be easier to achieve than an analogous $[C-C-C]^+$ array, presumably because Si−Si interactions can occur over greater distances than C−C interactions. This interpretation is supported by the theoretical finding[8] that a symmetric $[C-H-C-H-C]^+$ five-center four-electron σ-delocalized array has an overall length not much different from that of a proposed $[Si-Si-Si]^+$ three-center two-electron array. For that reason, we focus mainly on structures based on Si 3p orbitals in the σ-delocalized system, although we show that the same principles apply to systems using C 2p orbitals.

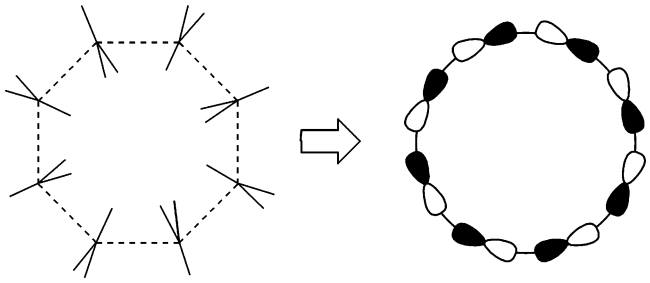

FIGURE 1. Arrangement for cyclic σ-bonding, using trigonal-planar groups (e.g., CH_3 and SiH_3) oriented to allow tangential p−p orbital overlap.

Experimental Section

Structures. All the structures considered in this paper are shown in Figures 2−4. Geometry optimizations were performed at the B3LYP/6-31G** level[9] using Jaguar 5.0[10] or Gaussian 98, revision A.9.[11] For structures **1**−**4**, it was necessary to employ symmetry constraints to maintain a cyclic array of planar CH_3 or SiH_3 units. Structures **5** (but not $\mathbf{5}^{2+}$) and **6** were found by vibrational frequency calculations to lie in minima of the potential surface (i.e., to have no imaginary frequencies).

(2) (a) Keith, T. A.; Bader, R. F. W. *Chem. Phys. Lett.* **1993**, *210*, 223. (b) Keith, T. A.; Bader, R. F. W. *J. Phys. Chem. A* **1993**, *99*, 3669. (c) Coriani, S.; Lazzeretti, P.; Malagoli, M.; Zanasi, R. *Theor. Chim. Acta* **1994**, *89*, 181. (d) Zanasi, R. *J. Chem. Phys.* **1996**, *105*, 1460. (e) Steiner, E.; Fowler, P. W. *J. Phys. Chem. A* **2001**, *105*, 9553. (f) Steiner, E.; Fowler, P. W. *Chem. Commun*., 2220. (g) Fowler, P. W.; Steiner, E. *Chem. Phys. Lett.* **2002**, *364*, 259.

(3) (a) Dewar, M. J. S. *Bull. Soc. Chim. Belg*. **1979**, *88*, 957. (b) Cremer, D. *Tetrahedron* **1988**, *44*, 7427. (c) Minkin, V. I.; Glukhovtsev, M. N.; Simkin, B. Y. *J. Mol. Struct.* **1988**, *50*, 93. (d) Cremer, D.; Gauss, J. *J. Am. Chem. Soc*. **1986**, *108*, 7467.

(4) (a) Paquette, L. A. *Angew. Chem., Int. Ed*. **1978**, *17*, 106. (b) Stahl, F.; Schleyer, P. v. R.; Jiao, H.; Schaefer, H. F., III; Chen, K.-S.; Allinger, N. L. *J. Org. Chem*. **2002**, *67*, 6599. (c) Williams, R. V. *Chem. Rev*. **2001**, *101*, 1185.

(5) (a) Houk, K. N.; Gandour, R. W. Strozier, R. W.; Rondan, N. G.; Paquette, L. A. *J. Am. Chem. Soc*. **1979**, *101*, 6797. (b) Havenith, R. W. A.; Fowler, P. W.; Jenneskens, L. W.; Steiner, E. *J. Phys. Chem. A* **2003**, *107*, 1867. (c) Jiao, H.; Schleyer, P. v. R. *J. Phys. Org. Chem*. **1998**, *11*, 655.

(6) (a) Hoffmann, R. *Solids and Surfaces: A Chemist's View on Bonding in Extended Structures*; VCH Publishers: New York, 1988; pp 3−14. (b) Atkins, P. W. *Quanta: A Handbook of Concepts*; Oxford University Press: Oxford, UK, 1991; pp 359−357. (c) Greenwood, N. N.; Earnshaw, A. *Chemistry of the Elements*, 2nd ed.; Butterworth Heinemann: Oxford, UK, 1991; p 1155.

(7) (a) Lipkowitz, K. B.; Larter, R. M.; Boyd, D. B. *J. Am. Chem. Soc*. **1980**, *102*, 85. (b) Paquette, L. A.; Usui, S. *Tetrahedron Lett.* **1999**, *40*, 3499. (c) Baldridge, K. K.; Leahy, J.; Siegel, J. S. *Tetrahedron Lett*. **1999**, *40*, 3503. (d) Livant, P. D.; Northcott, J.; Webb, T. R. *Book of Abstracts*; 219th ACS National Meeting: San Fransisco, CA, 2000. (e) Olson, L. P. *Org. Lett*. **2000**, *2*, 3059.

(8) Tantillo, D. J.; Hoffmann, R. *J. Am. Chem. Soc*. **2003**, *125*, 4042.

(9) (a) Becke, A. D. *J. Chem. Phys.* **2003**, *98* 5648. (b) Ditchfield, R.; Hehre, W. J.; Pople, J. A. *J. Chem. Phys*. **1971**, *54*, 724. (c) Hehre, W. J.; Ditchfield, R.; Pople, J. A. *J. Chem. Phys*. **1972**, *56*, 2257. (d) Gordon, M. S. *Chem. Phys. Lett*. **1980**, *76*, 167.

(10) *Jaguar 5.0*; Schrödinger, LLC: Portland, OR, 2002.

(11) Frisch, M. J.; Trucks, G. W.; Schlegel, H. B.; Scuseria, G. E.; Robb, M. A.; Cheeseman, J. R.; Zakrzewski, V. G.; Montgomery, J. A., Jr.; Stratmann, R. E.; Burant, J. C.; Dapprich, S.; Millam, J. M.; Daniels, A. D.; Kudin, K. N.; Strain, M. C.; Farkas, O.; Tomasi, J.; Barone, V.; Cossi, M.; Cammi, R.; Mennucci, B.; Pomelli, C.; Adamo, C.; Clifford, S.; Ochterski, J.; Petersson, G. A.; Ayala, P. Y.; Cui, Q.; Morokuma, K.; Malick, D. K.; Rabuck, A. D.; Raghavachari, K.; Foresman, J. B.; Cioslowski, J.; Ortiz, J. V.; Stefanov, B. B.; Liu, G.; Liashenko, A.; Piskorz, P.; Komaromi, I.; Gomperts, R.; Martin, R. L.; Fox, D. J.; Keith, T.; Al-Laham, M. A.; Peng, C. Y.; Nanayakkara, A.; Gonzalez, C.; Challacombe, M.; Gill, P. M. W.; Johnson, B. G.; Chen, W.; Wong, M. W.; Andres, J. L.; Head-Gordon, M.; Replogle, E. S.; Pople, J. A. *Gaussian 98*, revision A.9; Gaussian, Inc.: Pittsburgh, PA, 1998.

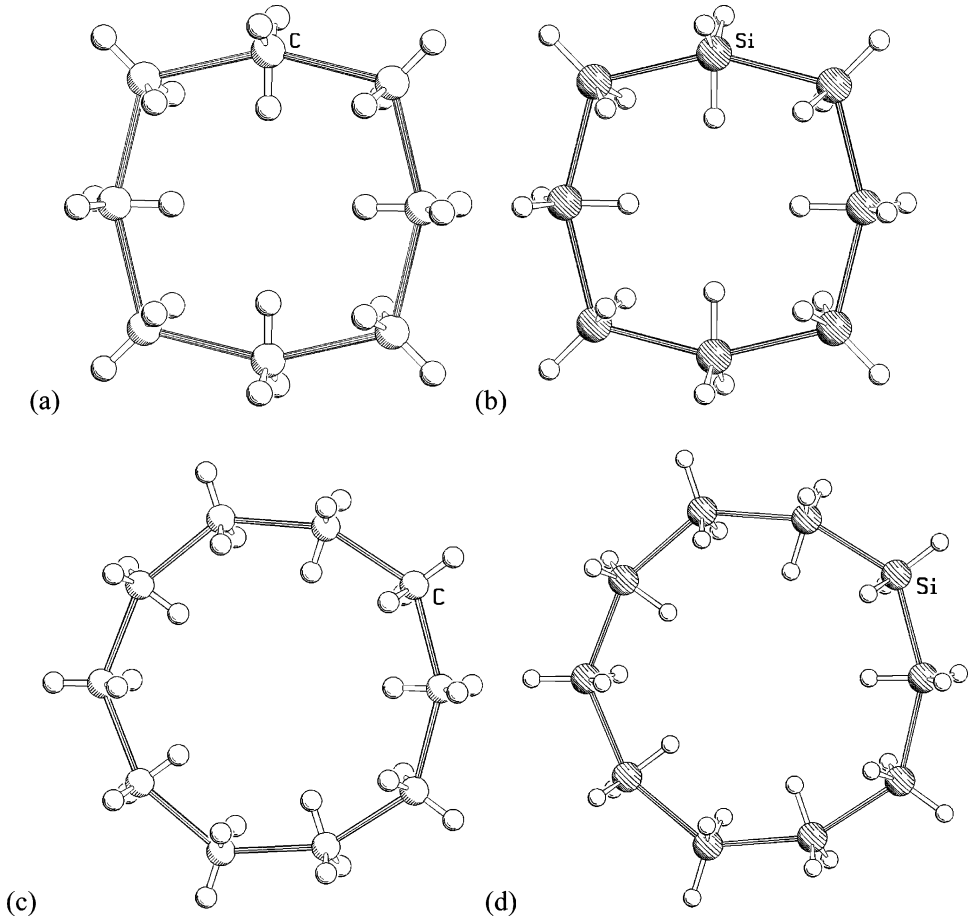

FIGURE 2. Model structures (a) **1**, (b) **2**, (c) **3**, and (d) **4**, optimized at the B3LYP/6-31G** level of theory. (Not shown are the very similar dicationic analogues $\mathbf{1}^{2+}$,... etc.). Symmetries are D_{4h} (**1** and **2**) and D_{5h} (**3** and **4**).

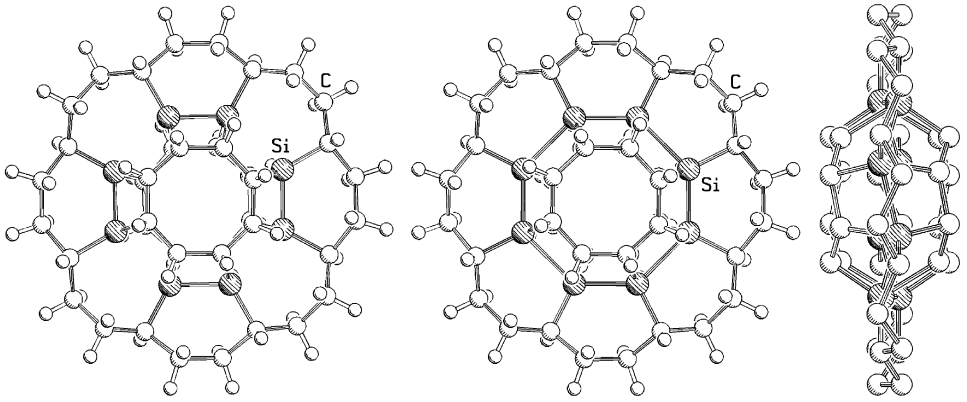

FIGURE 3. B3LYP/6-31G** optimized structures of **5** (D_4 symmetry), left, and $\mathbf{5}^{2+}$ (D_4 symmetry), center. A side view of $\mathbf{5}^{2+}$, with hydrogen atoms removed for clarity, is also shown on the right (the very similar side view of **5** is not shown).

Current Maps. Maps of current density induced by an external magnetic field were computed in the ipsocentric[2e,f] approach using the 6-31G** basis for the model systems $\mathbf{1}^{2+}$, $\mathbf{2}^{2+}$, $Si_{10}H_{30}^{4+}$ (structure $\mathbf{4}^{2+}$ in the +4 oxidation state), $\mathbf{5}^{2+}$ (six electrons in the tangential p−p σ-system), **2** (eight electrons), and **6** (10 electrons). In the ipsocentric approach, implemented in the SYSMO program,[12] also known by the acronym CTOCD−DZ (continuous transformation of origin of current density−diamagnetic zero), the induced current density at a given position is calculated with that point as the origin of vector potential. The maps were plotted in the plane of the central ring of heaviest atoms (or in the case of $\mathbf{5}^{2+}$ and **6**, in the median plane) and show the current induced by a magnetic field perpendicular to the plotting plane. Arrows represent the in-plane projections of the current density, and contours correspond to its total magnitude. Diamagnetic (≡ diatropic) circulation is shown as anticlockwise and paramagnetic (≡ paratropic) as clockwise.

(12) Lazzeretti, P.; Zanasi, R. *SYSMO package*; University of Modena, 1980; with additional routines for evaluation and plotting of current density by E. Steiner, P. W. Fowler, R. W. A. Havenith, and A. Soncini.

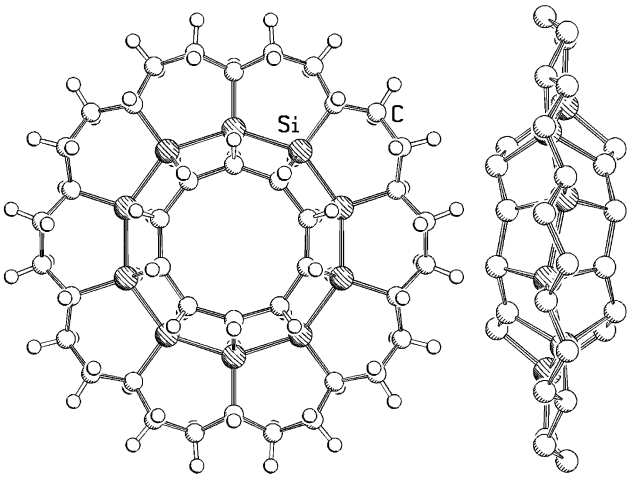

FIGURE 4. Front and side views of the B3LYP/6-31G** optimized structure of **6** (D_5 symmetry). The side view has had hydrogen atoms removed for clarity.

Results and Discussion

First, we present an overview of those orbital characteristics of tangential p−p bonding that may influence aromaticity. Next, we describe the specific molecular structures studied and finally discuss the computed ring currents for those structures.

Orbital Symmetry and Excitations of Cyclic σ-Bonded p Orbital Systems. The ipsocentric account of ring current in conventional π-monocycles[2f] relies on the connection between symmetry and angular momentum. Contributions to ring current arise from virtual excitations from occupied to empty orbitals. The product of orbital symmetries governs the type of ring current: if the product contains the symmetry of an in-plane translation, the contribution has a diatropic sense; if it contains the symmetry of the in-plane rotation, the contribution has a paratropic sense. If the product contains both symmetries, the contribution is of mixed character, often an indicator of localization of current. In the expression for the current, contributions are weighted by an energy denominator, and so it is the HOMO−LUMO and other frontier excitations that dominate the total valence current.[2e]

For π-conjugated monocycles in high symmetry, the frontier molecular orbitals can be classified by angular momentum, and the selection rules for diatropic/paratropic current can be translated into those terms. For the equilateral monocycle, an excitation that corresponds to a change of one unit angular momentum gives a diatropic current, whereas an excitation that corresponds to no change in angular momentum gives a paratropic current. For π-systems, this is effectively a node-counting argument: if the number of angular nodes changes by one from HOMO to LUMO, the excitation is translationally allowed; if it does not change, the excitation is rotationally allowed.

Thus, for a $(4n + 2)$ π-electron cycle of N atoms described in D_{Nh} symmetry, the only contribution to ring current arises from the HOMO−LUMO excitation, which corresponds to a translational transition and hence a four-electron diatropic current. In a lower point group, such as $D_{(N/2)h}$, extra transitions become allowed by symmetry. These include a rotational HOMO−LUMO transition and various other transitions of higher energy (see middle column of Figure 5). Where mixing of angular momentum remains small, these transitions will have a small probability and will not disturb the essential four-electron, diatropic nature of the ring current.

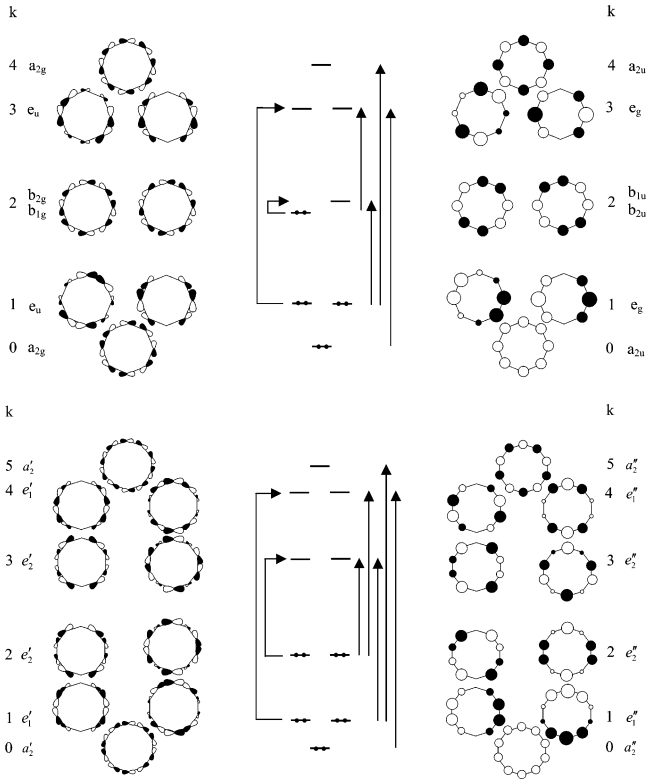

FIGURE 5. Molecular orbital and energy level diagram for cycles of eight and 10 atoms supporting π (right) and tangential (left) systems of p orbitals. Symmetries, labeled according to the point groups D_{4h} (eight-ring) and D_{5h} (10-ring), node counts (k), as defined in the text, and occupancy of charge-neutral systems are shown. The arrows denote the transitions from occupied to empty orbitals, which in the ipsocentric model determine the induced current: straight arrows indicate diatropic transitions allowed by translational symmetry, and bent arrows indicate paratropic transitions allowed by rotational symmetry.

For a $4n$ π-electron monocycle of N atoms, the maximum point group is again D_{Nh}, but in this symmetry, the system would have an open shell that would close on geometric distortion. In $D_{(N/2)h}$ symmetry, achieved, for example, by adopting bond or angle alternation or by rearrangement of attached groups, the HOMO and LUMO levels, corresponding to the same parent angular momentum in D_{Nh} symmetry, become nondegenerate, separated by a gap that is typically small. The HOMO−LUMO excitation is therefore rotationally allowed and is weighted by a small energy denominator, so that it gives rise to an intense two-electron paratropic ring current. Other transitions (e.g., HOMO−LUMO+1 and (HOMO-−1)−LUMO) become allowed by symmetry (Figure 5), but their contributions to the current are typically weaker.

The dichotomy between diatropic aromatic π-cycles and paratropic antiaromatic π-cycles is thus explained by the difference in the HOMO−LUMO symmetry product. Straightforward extension of this reasoning shows the pattern to be expected of tangential p−p σ-systems.

There is a one-to-one correspondence between π and tangential molecular orbitals of a cycle. Each p_π basis function is turned into a p_t basis function by local rotation of 90° about the radius vector. Such a rotation has the effect of interchanging every bonding and antibonding interaction along an edge of the

cycle. The energy level diagram is thereby exactly inverted. The sequence of filling of levels in both cases follows $k = 0, 1, 2,.., N/2$, where k is the number of nodal lines, counting only those lines that either cut through edges of the cycle or create zero coefficients on vertices. For a $(4n + 2)$ tangential system, the HOMO has $k = n$ and the LUMO $k = n + 1$; for a $4n$ system of π or tangential type, the HOMO and LUMO both have $k = n$. The correspondence carries over into orbital symmetries (see Figure 5). For the conventional π system, k is equivalent to an angular momentum quantum number Λ and orbital energy is increasing with Λ; for the tangential system, the orbital energy still increases with k, but now the angular momentum is $\Lambda = N/2 - k$, so that the energies in fact decrease with Λ.

The symmetry spanned by the whole π-basis and therefore the π-molecular orbital manifold is

$$\Gamma(\pi) = \Gamma(\sigma) \times \Gamma(T_Z)$$

where $\Gamma(\sigma)$ is the permutational representation of the vertexes of the cycle (with character $\chi_\sigma(R)$ equal to the number of vertices unshifted by operation R) and $\Gamma(T_Z)$ is the symmetry of the out-of-plane translation. This symmetry correspondence is at the heart of the pseudo-π-method for estimation of ring currents.[2g]

The basis of tangential p_t orbitals, and the set of MOs derived from them, spans

$$\Gamma(t) = \Gamma(\pi) \times \Gamma(\epsilon)$$

where $\Gamma(\epsilon)$ is the nondegenerate pseudo-scalar representation, with characters $+1$ under proper and -1 under improper operations. $\Gamma(\epsilon)$ represents a concerted local rotation at all vertices in a uniform sense and, for axial point groups, is a product of the symmetries in-plane rotation and out-of-plane translation

$$\Gamma(\epsilon) = \Gamma(R_Z) \times \Gamma(T_Z)$$

Therefore, π and tangential bases are related by a nondegenerate symmetry and, taking into account the inversion of the energy levels, we have

$$\Gamma_{\mathrm{HOMO}}(t) = \Gamma_{\mathrm{LUMO}}(\pi) \times \Gamma(\epsilon)$$

and

$$\Gamma_{\mathrm{LUMO}}(t) = \Gamma_{\mathrm{HOMO}}(\pi) \times \Gamma(\epsilon)$$

and therefore

$$\Gamma_{\mathrm{HOMO}}(t) \times \Gamma_{\mathrm{LUMO}}(t) = \Gamma_{\mathrm{HOMO}}(\pi) \times \Gamma_{\mathrm{LUMO}}(\pi)$$

This simple result for the symmetry product implies that the symmetry rules governing allowed transitions are exactly the same in π and tangential systems. A $(4n + 2)$ tangential cycle should have a four-electron diatropic ring current arising from translationally allowed HOMO−LUMO transitions, and a $4n$ tangential cycle should have a two-electron paratropic ring current arising from the rotationally allowed HOMO−LUMO transition. According to the ipsocentric orbital model, the magnetic criterion of aromaticity for tangential and π-systems should therefore follow the same Hückel rules.

Structures. The small model structures **1**−**4** (Figure 2) are constructed of planar CH_3 or SiH_3 groups arranged to form eight- or 10-membered rings in D_{4h} or D_{5h} symmetry with all-staggered hydrogens. This places all the heavy atoms in the same plane. In fact, the set **1**−**4** includes eight structures, each separately optimized in the 0 and +2 oxidation states (e.g., **1**, $\mathbf{1}^{2+}$, **2**, $\mathbf{2}^{2+}$...etc.). Table 1 gives selected data for these structures computed at the B3LYP/6-31G** level. The C−C distances are 0.4−0.5 Å shorter than the analogous Si−Si distances, whereas all C−H bond distances are about 1.09 Å and all Si−H bond distances about 1.46−1.47 Å. The eight-membered ring dications have six p electrons, and the 10-membered ring neutral molecules have 10 p electrons, and so they are potentially Hückel $4n + 2$ aromatic, whereas the eight-membered ring neutral molecules and 10-membered ring dications have eight p electrons and are potentially Hückel $4n$ antiaromatic. There is, however, no clear pattern of $4n + 2$ species having shorter C−C or Si−Si bonds than their $4n$ analogues. Less surprisingly, the C−C or Si−Si distances tend to be longer in the eight-membered rings than in the 10-membered rings, presumably due to angle strain. These simple structures provide a basis for several comparisons (C vs Si, eight-membered rings vs 10-membered rings, neutral species vs dications), as well as an uncluttered picture of the fundamental interactions.

TABLE 1. Selected Computational Results for Small Model Structures 1−4[a]

structure	B3LYP/6-31G** energy (Hartree)	C−C or Si−Si distance (Å)	C−C−C/Si−Si−Si angles (deg) (see diagram)
1, C_8H_{24}, D_4h	−318.76353	2.407	$A = 153.0$, $B = 117.0$
$\mathbf{1}^{2+}$	−318.24117	2.361	$A = 147.4$, $B = 131.1$
2, Si_8H_{24}, D_4h	−2329.99431	2.850	$A = 152.1$, $B = 117.9$
$\mathbf{2}^{2+}$	−2329.47407	2.884	$A = 149.2$, $B = 120.8$
3, $C_{10}H_{30}$, D_5h	−398.54196	2.368	$A = 150.9$, $B = 137.1$
$\mathbf{3}^{2+}$	−397.98572	2.339	$A = 151.9$, $B = 136.1$
4, $Si_{10}H_{30}$, D_5h	−2912.54935	2.825	$A = 152.3$, $B = 135.7$
$\mathbf{4}^{2+}$	−2912.00383	2.810	$A = 153.2$, $B = 134.8$

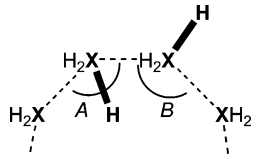

[a] The diagram shows the definition of the *A* and *B* angles, which vary depending on whether the in-plane X−H bond of the central heavy atom is directed into or out of the ring.

The large cage structure **5** was optimized in the 0 and +2 oxidation states (e.g., **5** and $\mathbf{5}^{++}$ (Figure 3)). As **5**, it is potentially eight-electron σ-antiaromatic, and as $\mathbf{5}^{++}$, it is potentially six-electron σ-aromatic. The hydrocarbon framework has two two-carbon bridges connecting adjacent pairs of Si atoms and one four-carbon bridge. Having bridges of different lengths results in bending into a cyclic structure, where the shorter bridges form the innermost portion and the longer bridges form the periphery. The resulting molecule resembles a wheel with spokes or, when viewed from the side, a flying saucer because it is thicker near the middle than at the edges. Figure 3 also shows that the Si atoms in $\mathbf{5}^{++}$ form a ring that zigzags above and below the mean plane of the molecule by ±0.26 Å. A feature of the framework surrounding the Si atoms is that the Si−Si distances can vary without disturbing the rotation axis (in the case of **5** and $\mathbf{5}^{++}$ a 4-fold axis) normal to this plane. In D_4 symmetry, the Si−Si distances alternate, but there is a possibility to reach D_{4d} symmetry with eight equivalent Si−Si distances. The neutral **5** optimizes to D_4 symmetry, with relatively pronounced Si−Si alternation (distances of 2.152 and

TABLE 2. Selected Computational Results for Large Framework Structures 5−6[a]

structure	method	energy (Hartree)	Si−Si distances (Å)	Si−Si−Si angle (deg)
5, $Si_8C_{40}H_{56}$, D_4[b]	B3LYP/6-31G**	−3873.311656	2.152, 2.731	128.8
5, C_1	HF/PM3	0.225381	2.342, 2.211[c]	132.6
5, D_4[b]	B3LYP/DGDZVP	−3873.190537	2.151, 2.747	128.9
$\mathbf{5}^{++}$, D_4[d]	B3LYP/6-31G**	−3872.879862	2.311, 2.488	128.2
$\mathbf{5}^{++}$, C_1	HF/PM3	0.782715	2.327, 2.328[c]	129.9
$\mathbf{5}^{++}$, D_4[d]	B3LYP/DGDZVP	−3872.746215	2.294, 2.534	128.5
6, $Si_{10}C_{50}H_{70}$, C_1	B3LYP/6-31G**	−4841.674999	2.182, 2.633[e]	136.8
6, D_5d[b]	HF/PM3	0.347004	2.261	141.6
6, C_2h[b]	B3LYP/DGDZVP	−4841.486812	2.376, 2.383[f]	137.4
6, C_2h[b]	B3LYP/LANL2DZ	−1985.011096	2.399, 2.405[g]	138.3

[a] Despite some Si−Si distance variation, all Si−Si−Si angle variations were insignificant, even in C_1 and C_{2h} symmetry. [b] After optimization in C_1 symmetry, the structure approached this point group very closely; the structure was then reoptimized using the stated symmetry. [c] Short/long Si−Si distances with insignificant variations from the stated values (i.e., close to D_4 symmetry for **5** and D_{4d} for $\mathbf{5}^{++}$). [d] At this level of theory, the structure collapsed to an oval-shaped structure with two separated charges when the symmetry constraint was removed. [e] Separately averaged short/long Si−Si distances; five distances from 2.181 to 2.183 Å and five from 2.629 to 2.637 Å. The symmetry was increased to D_5 to simplify the B3LYP/6-31G** SYSMO ring-current calculations. [f] Separately averaged short/long Si−Si distances; with six bonds from 2.376 to 2.377 Å and four at 2.383 Å. [g] Separately averaged short/long Si−Si distances; with six bonds from 2.398 to 2.399 Å and four at 2.405 Å.

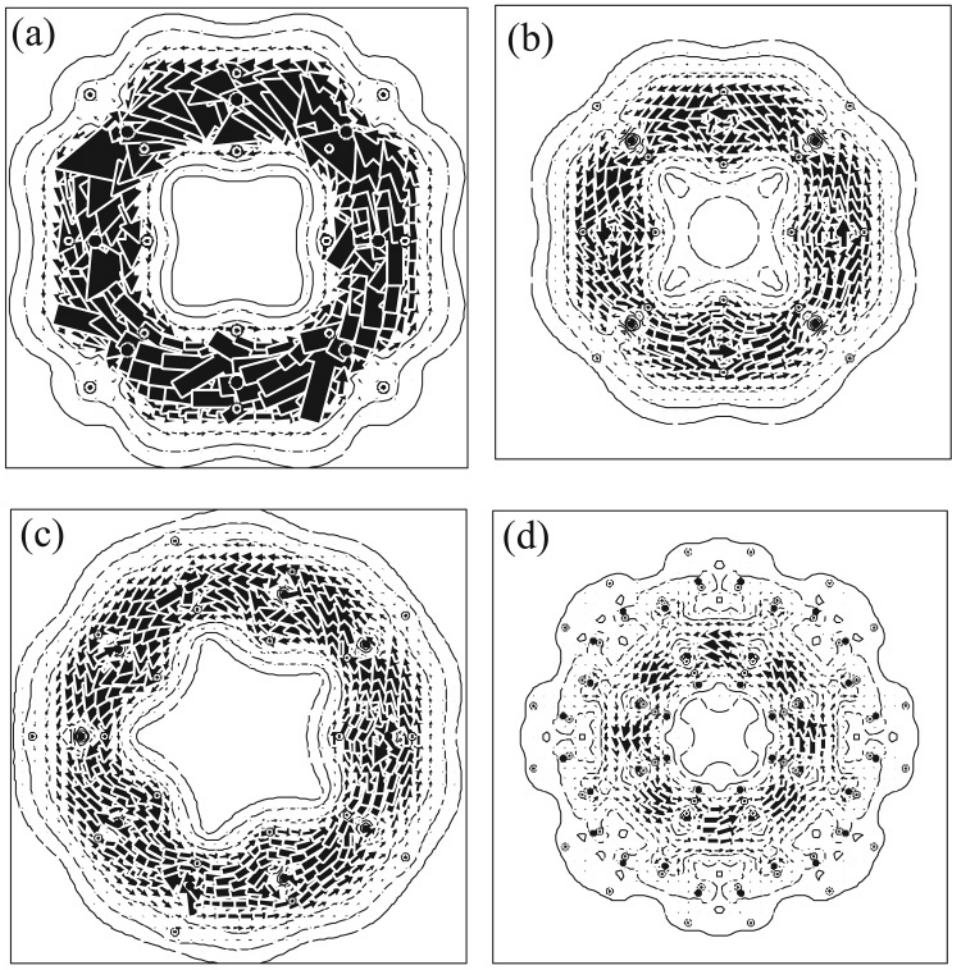

FIGURE 6. Comparison of HOMO contributions to current density induced by a perpendicular magnetic field in (a) $C_8H_{24}^{2+}$ ($\mathbf{1}^{++}$, D_{4h}, e_u HOMO), (b) $Si_8H_{24}^{2+}$ ($\mathbf{2}^{++}$, D_{4h}, e_u HOMO), (c) $Si_{10}H_{30}^{4+}$ (coordinates of $\mathbf{4}^{++}$ but in the +4 oxidation state, D_{5h}, e' HOMO), and (d) $Si_8C_{40}H_{56}^{2+}$ ($\mathbf{5}^{++}$, D_4, e_u HOMO). Current density is plotted in the plane of the carbon nuclei for $\mathbf{1}^{++}$, the plane of the silicon nuclei for $\mathbf{2}^{++}$ and $\mathbf{4}^{++}$, and the median plane of the silicon nuclei for $\mathbf{5}^{++}$, respectively.

2.731 Å) and hence three Si−C and one Si−Si bond per Si. In contrast, the optimization of $\mathbf{5}^{++}$ preserves D_4 symmetry, but with considerable reduction in the Si−Si distance (distances of 2.311 and 2.488 Å, cf. the σ-allyl cation[7e]), so that each Si appears to participate in three Si−C and two Si−Si bonds. This behavior could be explained in two different ways. One of these has to do with aromaticity, namely, that **5** avoids eight-electron antiaromatic character by localizing four Si−Si bonds and that $\mathbf{5}^{++}$ maximizes six-electron aromatic character by delocalizing Si−Si bonding. An alternative explanation is just that charge dispersal (not aromaticity) provides the driving force to delocalize Si−Si bonding in $\mathbf{5}^{++}$. The ipsocentric calculations help

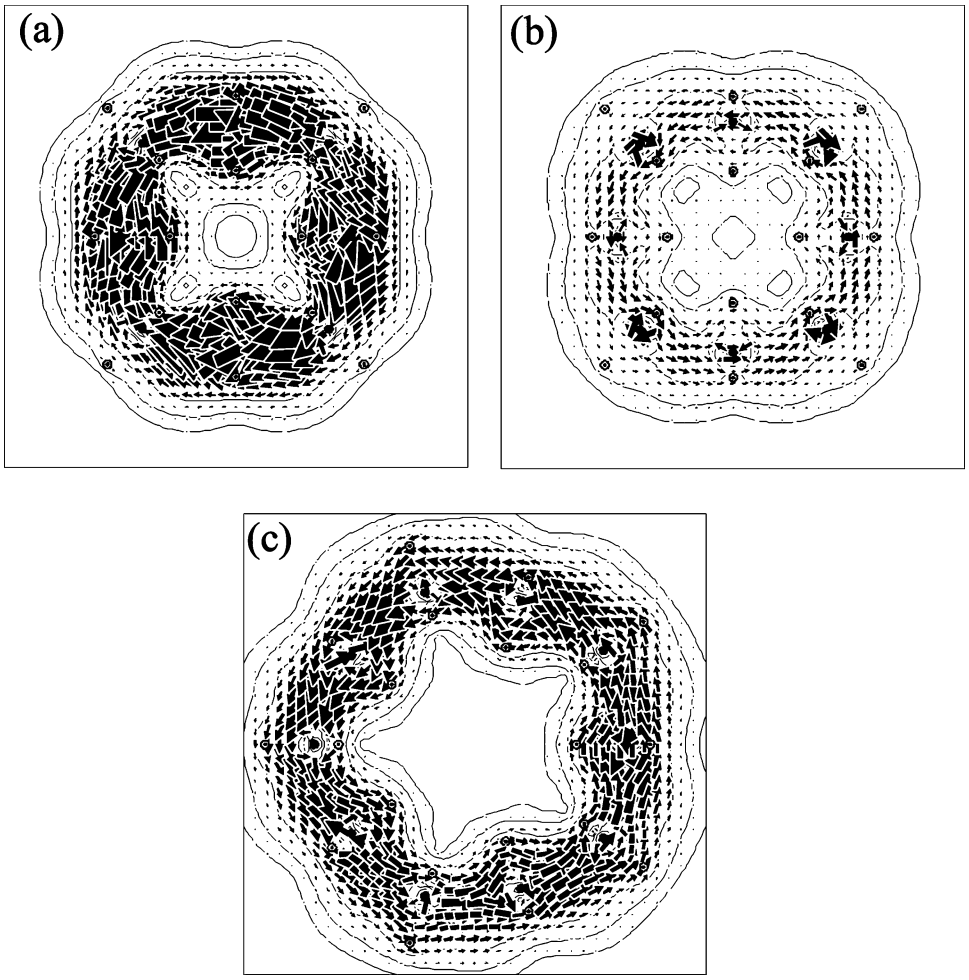

FIGURE 7. Orbital contributions to current density in contrasting paratropic and diatropic systems (a) and comparison of HOMO and HOMO-1 Si_8H_{24} (**2**, D_{4h}, b_{1g} HOMO) (b) and $Si_{10}H_{30}$ (**4**, D_{5h}, e'_1 HOMO) (c). Plotting conventions as in Figure 6.

us choose between these explanations, showing (vide infra) a diatropic ring current in $\mathbf{5}^{++}$.

Finally, there is structure **6**, where the same type of framework as in **5** is used to hold 10 silicon atoms in a ring. Again, one sees (Figure 4) the wheel-like flying saucer structure, and the Si atoms in **6** form a ring that zigzags above and below the mean plane of the molecule by ±0.25−0.26 Å. Significantly, in this case, a neutral molecule is potentially σ-aromatic without the need for symmetry constraints to hold the structure together. If σ-aromaticity is found in **6**, there will be no potential confusion with charge dispersal. A possibly important structural parameter for **6** is the degree to which the optimized structure approaches D_{5d} symmetry (10 equal Si−Si distances) versus D_5 or lower symmetry (alternating Si−Si distances). As shown in Table 2, the precise point group found for **6** varies from C_1 to D_{5d} depending on the method of calculation. Of several methods[13] tested for **6**, all but B3LYP/6-31G** predicted very little bond alternation.

Ring-Current Maps. Figures 6−8 show ring-current maps for selected model systems. In each case, a ring current is seen in the plotting plane and is dominated by the contribution of the HOMO electrons, occupying tangential p−p bonding orbitals. In most cases, only the map of the HOMO (or HOMO pair) is shown in the figure, but all-electron current maps and HOMO orbital contour plots are made available as Supporting Information (Figures S1−S6).

Model systems $\mathbf{1}^{++}$ (Figure 6a), $\mathbf{2}^{++}$, (Figure 6b), and $Si_{10}H_{30}^{4+}$ (Figure 6c) have six electrons in tangential orbitals and exhibit a pronounced diatropic current. The total current (Figures S1a, S2a, and S3a, Supporting Information) is essentially indistinguishable from the HOMO contribution (symmetry: e_u (D_{4h}) for $\mathbf{1}^{++}$ and $\mathbf{2}^{++}$ and e'_1 (D_{5h}) for $Si_{10}H_{30}^{4+}$).

The D_4 cage $\mathbf{5}^{++}$, in which a nonplanar ring of eight silicon atoms is clamped by a large carbon superstructure, shows an extended and complex pattern of total current in the median plane (Figure S4a, Supporting Information). The outer parts of this pattern are combinations of localized circulations in bonds. As the proposed tangential p−p σ-bonds between Si atoms are cut by the median plane, the central current vectors have a bunched appearance where they flow through the plotting plane alternately from above and below. The central region is dominated by the contribution of the e_u HOMO (Figure 6d), which accounts for essentially the whole of the all-electron current in that part of the molecule and has all the characteristics

(13) (a) Stewart, J. J. P. *J. Comput. Chem.* **1989**, *10*, 209. (b) Hay, P. J.; Wadt, W. R. *J. Chem. Phys.* **1985**, *82*, 270. (c) Wadt, W. R.; Hay, P. J. *J. Chem. Phys.* **1985**, *82*, 284. (d) Hay, P. J.; Wadt, W. R. *J. Chem. Phys.* **1985**, *82*, 299. (e) Godbout, N.; Salahub, D. R.; Andzelm, J.; Wimmer, E. *Can. J. Chem.* **1992**, *70*, 560.

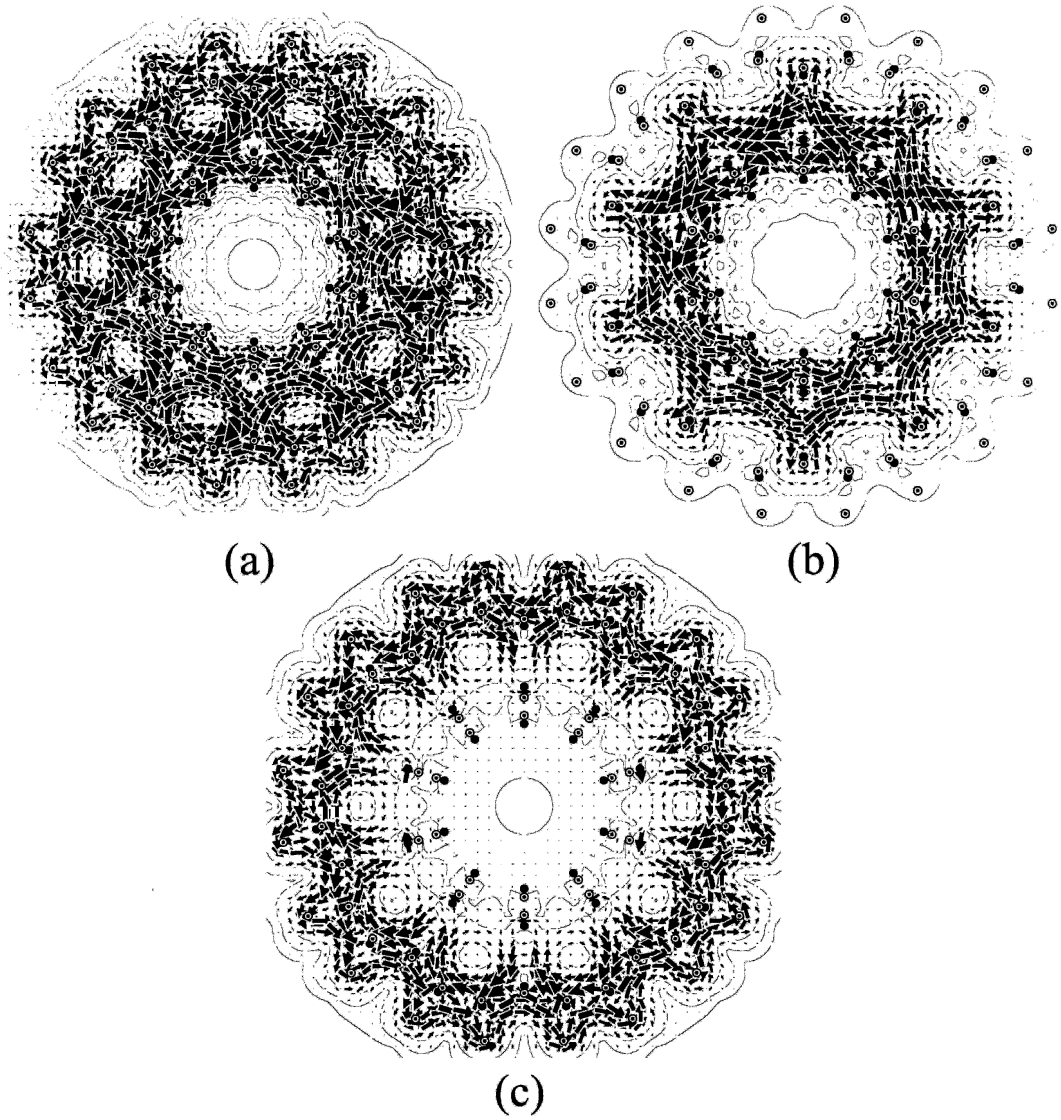

FIGURE 8. Comparison of (a) total (all-electron), (b) HOMO contribution, and (c) difference between total and HOMO contributions to current density induced by a perpendicular magnetic field in $Si_{10}C_{50}H_{70}$ structure **6** (idealized to D_{5h} symmetry). The plotting plane here is the median plane of the silicon atoms. Other plotting conventions are as in Figure 6.

of a four-electron HOMO−LUMO diatropic ring current, as expected for an aromatic six-electron system.

Si_8H_{24} (**5**) has eight electrons in tangential Si−Si bonding orbitals with a b_{1g} HOMO and b_{2g} LUMO; there is a pronounced paratropic ring current (Figure S5a, Supporting Information), which is dominated by the two electrons of the HOMO (Figure 7a), opposed by a weak diatropic contribution from the e_u HOMO−1 orbital pair (Figure 7b).

$Si_{10}H_{30}^{2+}$ at the equilateral D_{5h} geometry would have an $(e'_2)^2$ open shell. However, with tetra-cationic and neutral electron counts, and retaining the geometry of the dication, $Si_{10}H_{30}^{4+}$ (Figure 6c) and $Si_{10}H_{30}$ (Figure 7c) both show diamagnetic, HOMO-dominated ring currents. All electron current density maps and orbital contour plots for $Si_{10}H_{30}^{4+}$ and $Si_{10}H_{30}$ are shown in Figures S3 and S6 (Supporting Information).

$Si_{10}C_{50}H_{70}$ (**6**) has D_{5d} symmetry and 10 electrons in tangential Si−Si bonding orbitals with an e_{2u} HOMO pair and e_{2g} LUMO pair. The total current pattern in the median plane of the molecule shows overall diatropic flow (Figure 8a), although with returns and eddies in the region of the supporting carbon framework. However, as expected from the electron count, orbital analysis shows that there is a pronounced HOMO diatropic ring current (Figure 8b) running around the central silicon crown and following the lines of the Si−Si σ-bonds. The intensity of this σ-current expressed as the maximum of the current density per unit inducing field is 0.107 au (where the benzene π-current at 1 a_0 above the molecular plane is 0.08 au). The 100 core orbitals make essentially no contribution to the map in this plane. Contributions from the other occupied orbitals are individually small but sum up to a pattern of circulation outside the silicon center of the cage—as shown by the analysis of total induced current density into HOMO and HOMO complement contributions in Figure 8.

Conclusion

To summarize, we see that the orbital symmetry rules established for tangentially p−p bonded σ-delocalized systems account for all observations. $\mathbf{1}^{++}$, $\mathbf{2}^{++}$, $Si_{10}H_{30}^{4+}$ (derived from $\mathbf{4}^{++}$), $\mathbf{5}^{++}$, and **6** are $(4n + 2)$ systems and indeed are diatropic

with a HOMO dominated four-electron ring current. The orbital contribution and the total current density are almost indistinguishable in the region of the ring of heavy atoms. Compound **2** is a 4*n* system and again shows the features expected from the model: a paratropic total current, domination by the two-electron HOMO contribution, and an opposing but weak diamagnetic current arising from the four electrons of the HOMO−1 level. These results are all fully in line with a Hückel-like rule for electron counts of the p−p bonding subsystem: $(4n + 2)$ cases show diatropic and $(4n)$ cases paratropic ring currents, indicating aromaticity/antiaromaticity in the magnetic criterion. The ipsocentric approach[2e,f] gives a partition of total magnetic response into physically nonredundant orbital contributions and gives an explanation of these results in terms of pictorial molecular orbital theory and symmetry-based selection rules.

If aromaticity is measured on the magnetic criterion, the present calculations indicate that consideration of tangential p−p overlap of Si atoms can be used to design σ-aromatic systems. Structure **6** is a particularly notable example of this, showing a σ-aromatic ring current despite the absence of charge(s) that might tend to aid electron delocalization (as is presumably the case with $\mathbf{5}^{++}$). The superstructure used in $\mathbf{5}^{++}$ and **6** was not the result of extensive design studies, so it may be far from optimal for encouraging σ-aromatic overlap; but given the internuclear Si−Si distances involved in this case, it is unclear how readily σ-aromaticity via tangential p−p bonding might be achieved using C instead of Si. However, an alternative strategy using H atoms to bridge gaps between C atoms[8] might result in interesting σ-aromaticity of hydrocarbons, based on tangential overlap of C 2p orbitals with H 1s orbitals.

Acknowledgment. Financial support is gratefully acknowledged for P.W.F. (Royal Society/Wolfson Research Merit Award Scheme), M.L. (EPSRC DTA award), and A.R. (British-Council/Polish Academy of Sciences and EU FP5 Research Training Network FAMOUS CT-2002-00171)

Supporting Information Available: B3LYP/6-31G** optimized Cartesian coordinates for all structures. Current density maps (all electron maps and HOMO contributions) and orbital contour plots for structures $\mathbf{1}^{++}$, $\mathbf{2}^{++}$, $\mathbf{4}^{++}$, $\mathbf{5}^{++}$, **2**, and **4**. This material is available free of charge via the Internet at http://pubs.acs.org.

JO060788P